III. Degradation of methyl orange and rhodamine B by using novel nano MgO/ZnO catalyst

3.1 Introduction

Contamination of water and air due to organic matter poses severe threat to life on the earth [1]. The presence of such matter increases the environmental pollution. Degradation of such pollutants becomes the need of the hour to minimize the pollution. Use of semiconductors for photocatalytic activity has attracted attention as they potentially degrade the organic pollutants in water and air [1-5]. Irrespective of the types and activities of semiconductors, photocatalytic reactions can work at ambient conditions, without producing any additional pollutant [6].

The general scheme for the photocatalytic destruction of organic compounds involves the following three steps:

(i) when the energy hυ of a photon is equal to or higher than the band gap (Eg) of the semiconductor, an electron is excited to conduction band, with simultaneous generation of a hole in the valance band;

ii) then the photoexcited electrons and holes can be trapped by the oxygen and surface hydroxyl, respectively, and ultimately produce the hydroxyl radicals (•OH), which are known as the primary oxidizing species; and

(iii) the hydroxyl radicals commonly mineralize the adsorbed organic substances.

Among all, TiO_2 is the most extensively studied photocatalyst. It showed relatively higher photocatalytic activity and is stable to incident photon or chemical corrosion [4, 7-8]. Next to TiO_2, ZnO is the widely used photocatalyst for degradation of organic pollutants. ZnO is n-type semiconductor and has the similar band gap as TiO2 (ZnO- 3.4 and TiO_2 3.2 eV). The added advantage of ZnO over TiO_2 is that, it absorbs over a larger fraction of the UV spectrum having threshold wavelength of 387 nm [9]. Gauvea et. al. had studied photocatalytic activity of ZnO for degradation of different reactive dyes and was found to be having very good photocatalytic activity [10]. Lizama et. al. had used ZnO suspension for degradation of reactive blue 19[11]. S. Amisha et. al. showed photocatalytic activity of ZnO for photodegradation of reactive black 5[12].

However, the photoexited electrons and holes can also recombine to reduce photocatalytic activity of the semiconductor. This problem can be rectified by modifying the catalyst with the other metal.

The use of other semiconductor with TiO_2 improves the charge separation and hinders the charge recombination [13-17]. The 3% MgO on TiO_2 was effectively used for degradation of Eosin Y dye. In this case, the thin layer of insulating MgO on TiO_2 acts as a barrier for charge recombination. The charge recombination rates were progressively reduced with the small amount of MgO present on TiO_2. Therefore, the presence of MgO layer on TiO_2 slows down the charge recombination [13].

Methyl orange (MO) and rhodamine B (RB) (figure 3.1) are water soluble dyes which are widely used in textile, printing, paper, pharmaceutical and food industries [18,19]. In the present study, we carried out photodegradation of methyl orange and rhodamine B dyes using MgO/ZnO nano catalyst. Effect of various parameters such as loading of MgO on ZnO, amount of photocatalyst used, initial concentration of dye, effect of pH and effect presence of various anions on photodegradation was studied.

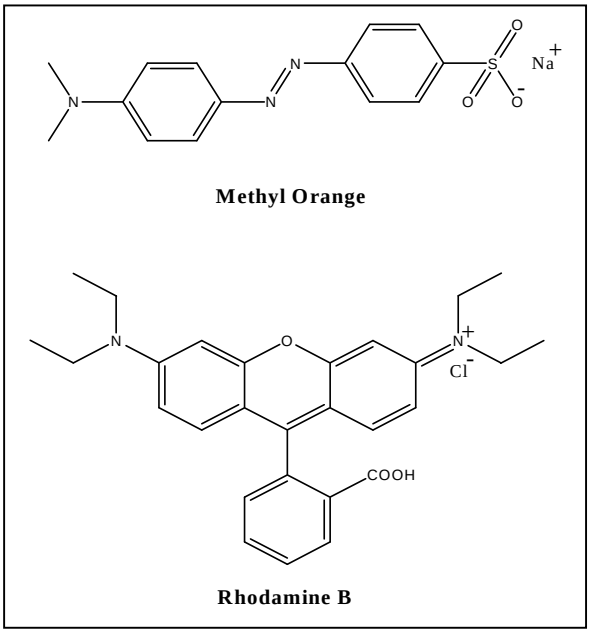

Figure 3.1 Structure of Methyl Orange (MO) and Rhodamine B (RB)

Rong Chen et. al. reported microwave assisted facile and rapid method for the synthesis of bismuth phosphate ($BiPO_4$) nanostructures and its photocatalytic application on the degradation of methyl orange (MO) under UV and visible light irradiation [20]. Yong Cai Zhang and co-workers reported hydrothermal synthesis of SnS_2 nanoparticles. The structure, composition and optical property of the resultant SnS_2 were characterized by XRD, TEM, EDS, X-ray photoelectron spectroscopy (XPS). The photocatalytic activity of SnS_2 was tested on the degradation of methyl orange (MO) in distilled water under visible light ($\lambda > 420$ nm) irradiation. The photocatalytic activity of SnS_2 nanoparticles show a promising visible light-driven remediation of water polluted by the chemically stable MO dye [21].

Feng Chen et al. reported application of Ag-loaded brookite/anatase photocatalyst prepared via an alkalescent hydrothermal process for degradation of methyl orange (MO). The catalysts were characterised with XRD, BET and HRTEM techniques. They showed that 2.0 mol% of Ag with TiO_2 increases the photocatalytic degradation of MO 2.28 times as compared with Degussa TiO_2 [22]. Luminita Andronic et. al. reported new photocatalytic materials, based on copper sulphides (CuxS powder and film) and CuxS/TiO2 nanocomposite films with enhanced degradation efficiency of MO dyes under UV and visible light irradiation. The dye degradation efficiency of copper sulphide powder was lower than the $CuxS/TiO_2$ film due to the opacity of the suspensions. The $CuxS/TiO_2$ composites show higher activity than compared with the activity of CuxS and TiO_2. The photocatalytic experiments demonstrated that the CuxS/TiO2 hybrid photocatalyst activated with H_2O_2 exhibited a higher catalytic efficiency (99%) for degradation of dyes than the mono-component films [23].

Dai Hongxing and co-worker have synthesised $BiVO_4$ having various morphologies. This photocatalyst has lowest band gap energy and gave the best photocatalytic performance for the degradation of MO under visible-light illumination. They also correlate the photocatalytic activity of the $BiVO_4$ material with its morphology [24]. Haijiao Zhang and group prepared the TiO_2/graphene composite catalysts. They have confirmed that electron beam irradiation pretreatment of graphene could significantly enhance the photocatalytic activity of TiO_2 in the degradation of methyl orange [25].

Yang Hou and group have prepared spinel $ZnFe_2O_4$ nanospheres by one-step, template-free solvothermal method. The prepared $ZnFe_2O_4$ nanospheres showed outstanding advancement over ZnFe2O4 nanoparticles in photocatalytic degradation of rhodamine B (RhB) under Xe lamp irradiation [26]. Won-Chun Oh et. al. have prepared carbon 60 (C60) coupled CdS-TiO_2 system for degradation of rhodamine b. The addition of C60 to CdS/TiO_2 system can enhance the catalytic activity. Increase in the content of CdS in C60 and TiO_2 can enhance the catalytic activity. These were because CdS improving the reaction state produces more charge and decreased the recombination rate of electron–hole pair [27].

Kan Zhangc and co-worker presented the synthesis and characterization of reduced graphene oxide–TiO_2 (RGO–TiO_2) nanocomposite derived from commercial P25 and graphene oxide (GO) via a facile hydrothermal reaction. This nanocomposite has high surface area, excellent structure, and great electrical and optical properties. They proved that the photocatalytic activity of prepared catalyst was higher than that of a commercial P25 under UV and visible light irradiation for degradation of RhB [28].

Jungang Hou and co-workers synthesised $BiTiO_2$ and PANI/Bi/TiO_2 by template-free hydrothermal method. The photocatalytic activity of prepared catalyst was tested on degradation of rhodamine b. It was observed that 0.5% of PANI

increased the photocatalytic activity of Bi/TiO_2 under visible-light irradiation (λ > 420 nm). The photocatalytic efficiency was also improved by the appropriate hydroxyl radical concentration generated by H_2O_2 [29]. Rajesh J. Tayade et. al. have used TiO_2 with UV-LED as an irradiation source for photocatalytic degradation of RhB dye in aqueous medium. They also studied the effect of various metal ions such as Zn^{2+}, Ag^{+}, Fe^{3+}, Cu^{2+} and Cd^{2+} on the photocatalytic degradation of RhB. The possible mechanism proposed for the photocatalytic degradation of RhB dye under UV-LED irradiation light was based on electrospray ionization mass spectrometry (ESI-MS) analysis. They showed the UV-LED may be a good alternative source for conventional UV sources [30].

Abbas Mehrdad and group studied the kinetics of the degradation of Rhodamine B in presence of hydrogen peroxide and oxides of aluminium and iron. The obtained results showed the efficiency of the examined systems for the degradation of Rhodamine B, (FeO +H_2O_2) > (nano-sized Al_2O_3 + H_2O_2) > (Al_2O_3 + H_2O_2) > (H_2O_2) [31].

Chenguo Hu and co workers reported that photocatalytic removal of rhodamine B (RhB) and methyl orange (MO) by using the hierarchical SnO_2 nanoflowers and SnO_2 nanorods under sunlight. The hierarchical SnO_2 nanoflower catalyst showed higher photocatalytic activity as compared with SnO_2 nanorod catalyst [32]. Fengqiang Sun et. al. reported a novel spindly CuO prepared by the hexamethylenetetramine (HMTA) assisted solution process at low temperature (<95 ◦C). The prepared CuO photocatalyst exhibited high photocatalytic activity in the degradation of dye pollutants, including rhodamine B (RhB), methyl orange (MO), methylene blue (MB) and erosin B, in the presence of a small amount of H_2O_2 under irradiation by a low-power (100 W) halogen tungsten lamp [33].

OH Won-Chun et. al. have prepared graphene-CdSe composite by a simple hydrothermal method. The photocatalytic activity of the graphene-CdSe composite was investigated by the degradation of MB, MO, and Rh.B in aqueous solution

under UV or visible light irradiation [34]. Shifu Chen and co-worker synthesised $AgBr/H_2WO_4$ photocatalyst by deposition–precipitation method. The $AgBr/H_2WO_4$ showed excellent performance on the degradation of MO and RhB and higher photocatalytic activity than single AgBr or H_2WO_4 under visible-light irradiation ($\lambda > 420$ nm) [35].

In all above reported work, various kind of mixed metal oxides were used for degradation of methyl orange and rhodamine b. In this work, we tested the photocatalytic activity of MgO/ZnO degradation of methyl orange and rhodamine b. Different operational parameters such as effects of MgO concentration on degradation, catalyst concentration, different initial concentration of dyes on initial rate of degradation, effect of initial pH and effect of presence of different anions on degradation were studied.

3.2 Experimental

3.2.1 Materials

Methyl orange and rhodamine B of analytical grade were purchased from M/S S.D. Fine Chemical, Mumbai, India. All other reagents were of analytical grade and were used without any further purification.

3.2.2 Methods

3.2.2.1 Synthesis of nano ZnO and MgO/ZnO

Zinc acetate was used as precursor for the preparation of ZnO nanoparticles. In a typical procedure, 0.82 g of zinc acetate was dissolved in solution of 50 cm^3 of methanol and 300 cm^3 of distilled water. The solution of 0.3 g of sodium hydroxide in 30 mL of methanol was used for precipitation of zinc hydroxide under vigorous stirring. The resulting solution was then filtered off. The obtained precipitate was washed with water and then with methanol. The powder was dried at 120^oC and subsequently calcined at 400^oC for 3 hrs. Various catalysts of 1%, 3%, 6% and 9% MgO with ZnO were prepared by adding appropriate amount of magnesium acetate in the original solution of zinc acetate before precipitation.

3.2.2.2 Preparation of Dye solutions

Individual stock solutions of 500 ppm of methyl orange and rhodamine b were prepared by dissolving 500 mg of dyes in 1000 mL of distilled water. Various concentrations for degradation study were prepared from the stock solutions.

3.2.2.3 Photodegradation experiment

Photodegradation experiments were carried out in a cylindrical reactor (**Chapter 2, Figure 2.2**). The reactor was a simple cylindrical tube like a measuring cylinder with outlet provided at the top to withdraw samples at specific time intervals without disturbing the reaction system. The cylinder was surrounded by a cooling jacket to maintain the reaction temperature constant during reaction, as the heat is generated because of irradiation. Reaction mixture was stirred magnetically

using a Teflon coated stirrer magnet. The radiation sources used were a low pressure mercury vapour lamp (Philips, UV-C, 16 W) emitting ultra violet radiation. After specific time intervals samples were collected by means of suction bulb from the sample outlet and further analysed.

Experiments were carried out with 300 mL of the dye solution of desired concentration (*Co* = 10 mg/L) prepared in the double distilled water was taken. A known amount of photocatalyst was added in solution. Irradiation was carried out by using a 16 W low pressure mercury lamp (Philips UV-C). Few mL of sample solution was collected before and at regular intervals for analysis during irradiation. Catalyst was removed by centrifugation.

3.2.2.4 Analysis

The degradation of dye was monitored by measuring the absorbance of respective dyes UV-VIS spectrophotometer (Shimadzu 1650 model). Degradation of methyl orange was monitored at 463 nm and rhodamine b at 554 nm.

3.2.2.5 Kinetic Measurement

In a photodegradation kinetic measurements, 300 mL of the dye solution of various concentration were prepared in the double distilled water was taken. A known amount of nano photocatalyst was added in solution. Irradiation was carried out by using a 16 W low pressure mercury lamp. Few mL of sample solution was collected before and at regular intervals for analysis during irradiation. Catalyst was removed by centrifugation. The absorbance of the dye was measured colorometrically. The plot of ln(C/Ct) Vs t was plotted to determine initial rate of the reaction.

3.2.3 Characterization of ZnO and MgO/ZnO

3. 2.3.1 X-Ray Diffraction

The X-ray diffractograms were obtained (XRD, MINI FLEX RIGAKU MODEL) with Cu K-α radiation (1.5418 A°) with scanning rate of 2^o per min from 2^o to 80^o. XRD patterns of ZnO and MgO/ZnO were shown in fig. 3.2 which was calcined at 400^oC for 3 hrs. The hexagonal close packed structure of prepared powder was observed. The diffraction peaks displayed almost all the characteristic diffractions corresponding to wurtzite structure of ZnO, matching with the JCPDS pattern (PDF: #75-0576). It was found that the prepared nanoparticles show good crystallinity. The spectrum did not show peak for MgO as its concentration in the prepared catalyst was very low. The spectrum did not give the extra peak for mixed metal oxide of MgO and ZnO, which indicates that no composite metal oxide was formed.

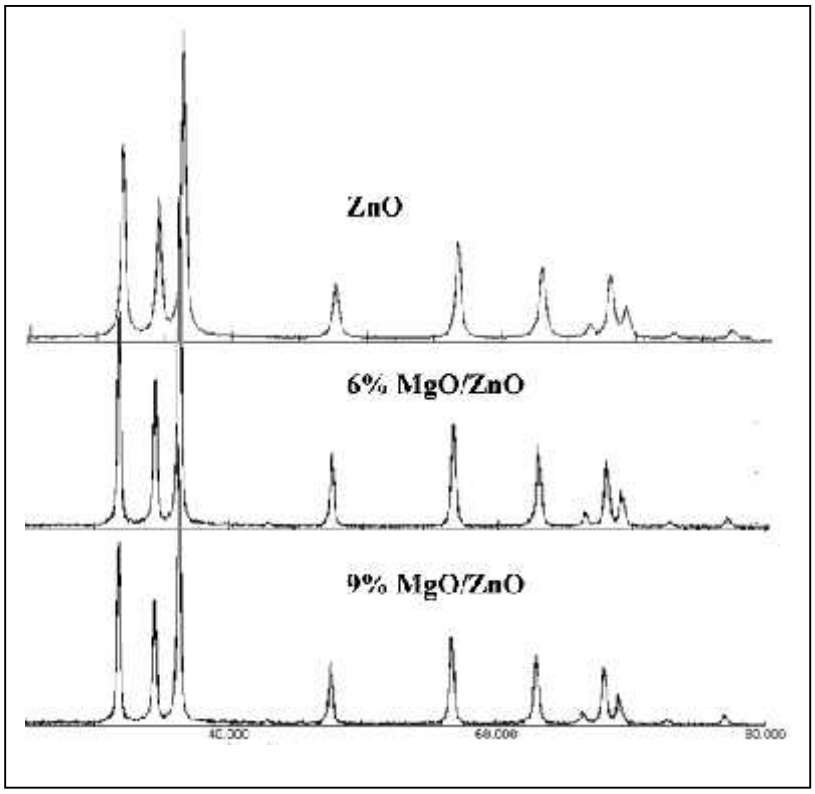

Figure 3.2 XRD of Nano ZnO and MgO/ZnO

3.2.3.2 Transmission, Scanning Electron Microscope and EDAX

Particle size and external morphology of the prepared particles were observed on a Transmission Electron Microscope (TEM) (Philips CM 200, operating at 20 – 200 kV accelerating voltage and having resolution up to 2.4 A^o). Surface morphology and EDAX (Energy Dispersive X-Ray Spectroscopy) analysis was done by using Field Emission Gun-Scanning Electron Microscopes (FEG-SEM) JSM-7600F model operating at accelerating voltage 0.1 to 30 kV, Magnification x25 to 1,000,000 and having resolution 1.0 nm - 1.5 nm (15kV). Figure 3.3 shows the TEM image and figure 2.4 shows the SEM image of ZnO particles. The TEM and SEM images shows the particles are in nano region.

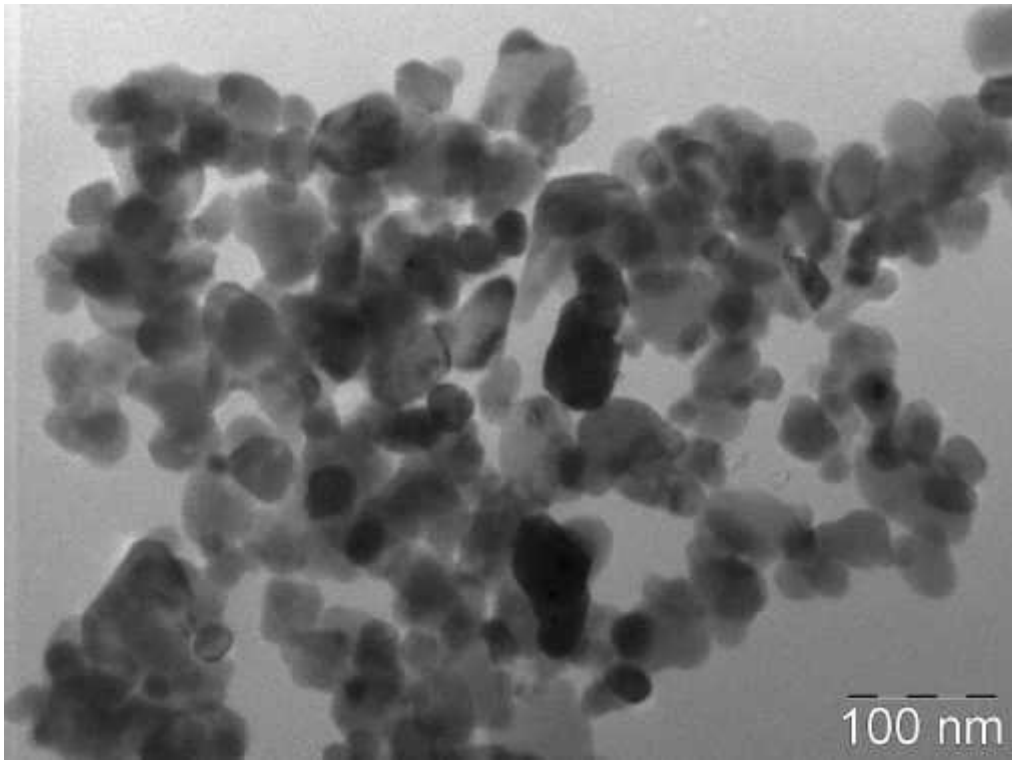

Figure 3.3 TEM image of Nano ZnO

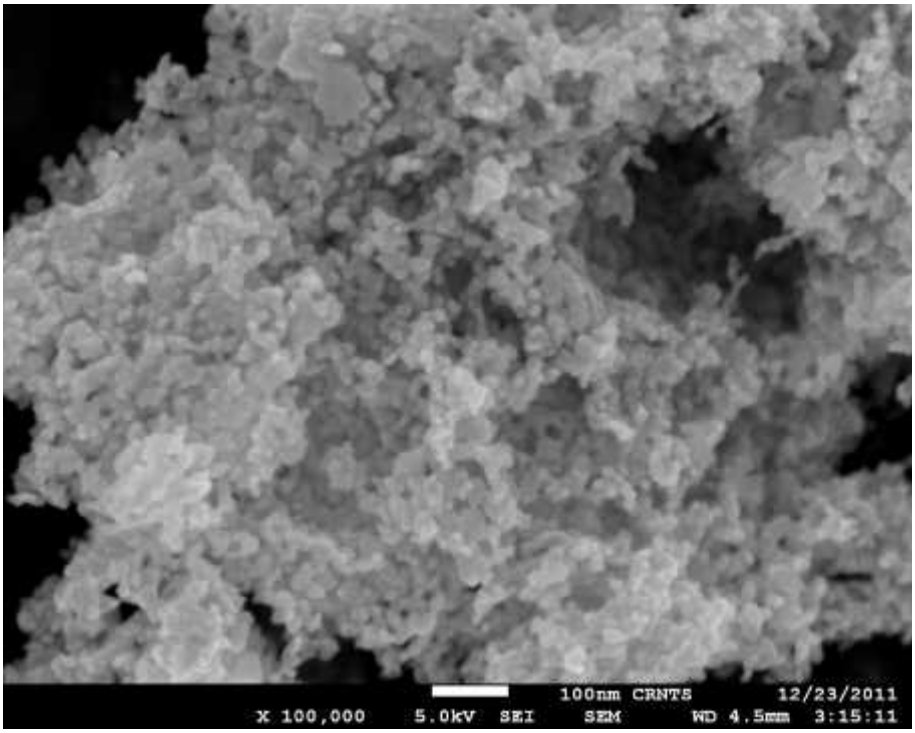

Figure 3.4 SEM image of Nano ZnO

SEM images of 1%, 3%, 6% and 9% of MgO with ZnO were shown in fig. 3.5. All prepared catalysts are formed in nano sized region. EDAX images of prepared MgO/ZnO shown in figure 3.6 which shows presence of only zinc, oxygen and magnesium elements (with increased concentration). The percentage compositions of the elements present in the catalyst are summarized in table 3.1.

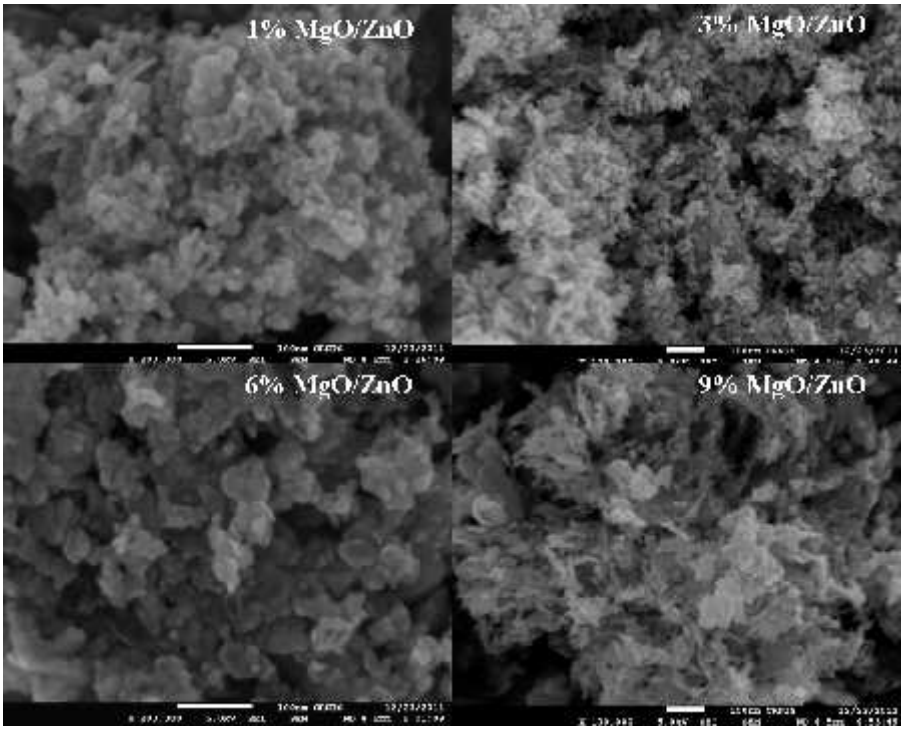

Figure 3.5 SEM images of 1%, 3%, 6% and 9% MgO/ZnO

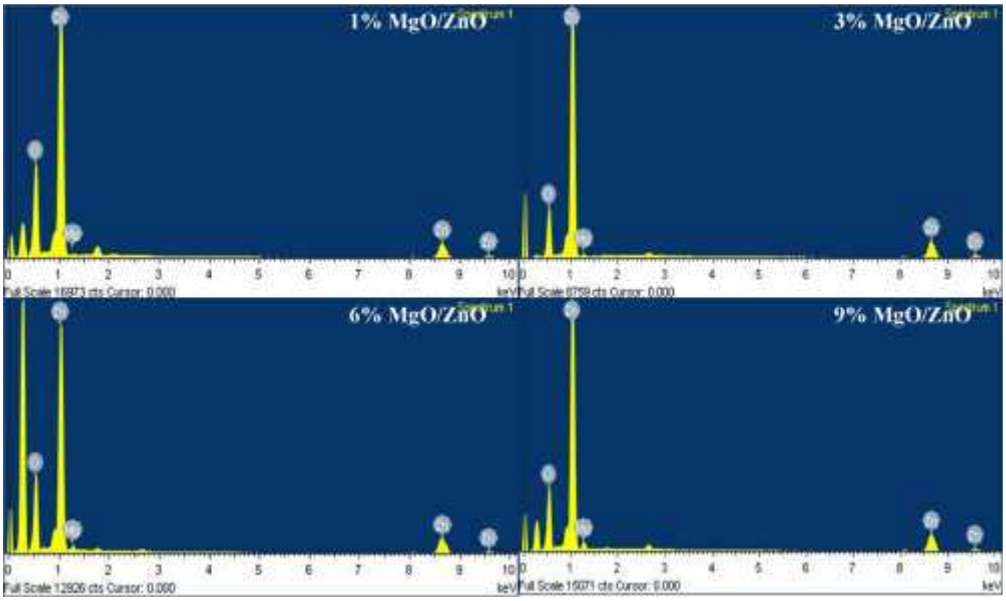

Figure 3.6 EDAX images of 1%, 3%, 6% and 9% MgO/ZnO

Table 3.1. Atomic weight % of elements in prepared catalyst

Catalyst	**Elements (Atomic Weight %)**		
	Zn	**Mg**	**O**
ZnO	80.24	00	19.76
1% MgO/ZnO	79.60	0.44	19.96
3% MgO/ZnO	78.31	1.8	19.88
6% MgO/ZnO	75.90	3.6	20.49
9% MgO/ZnO	73.48	5.4	21.11

3.3 Result and Discussion

3.3.1 Effect of MgO with ZnO

Number of duplicate experiments was carried out by using 50 mg of catalyst for degradation of 10 ppm solution of MO and RB dyes. Figure 3.7 A and 3.7 B shows that 3% of MgO with ZnO was the most suitable catalyst for degradation of methyl orange and rhodamine b dyes. 3% of MgO with ZnO showed similar photocatalytic behaviour like 3% of MgO/TiO_2 used for degradation of Eosin Y [13].

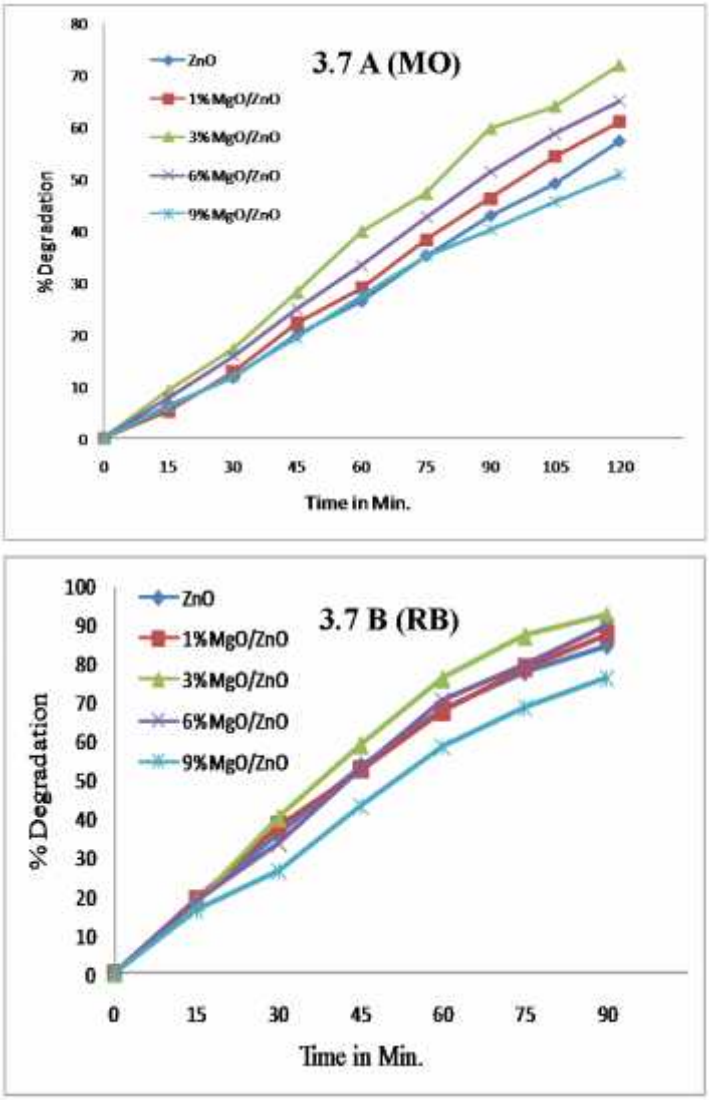

Figure 3.7 Effect of presence of MgO on degradation of MO and RhB

3.3.2 Effect of catalyst concentration on degradation of dyes

The effect of catalyst concentration on the degradation of dyes MO and RB were investigated by employing different initial concentration of 3% MgO/ZnO, varying from 0 to 150 mg and with and without air purging. In case of methyl orange 50, 100 and 150 mg of 3% MgO/ZnO gave 41%, 39% and 38% degradation respectively in first 60 min. whereas in case of rhodamine 50, 100 and 150 mg of 3% MgO/ZnO gave 78%, 75% and 77% degradation respectively in first 60 min. The results are summarized in table 3.2. The high degradation rate was observed with 50 mg of the catalyst without air purging for both MO and RB. The data shows that the photo-degradation did not increase with increase in catalyst concentration. The purging of air did not have any additional effect on the degradation rate.

Table 3.2. Influence catalyst concentration on degradation of MO and RB

Catalyst concentration	Dye			
	MO		RB	
	k (min^{-1})	R	k(min^{-1})	R
00	0.021	0.963	0.069	0.987
Air	0.048	0.981	0.077	0.984
50 mg	0.149	0.988	0.372	0.954
50 mg + Air	0.125	0.977	0.355	0.969
100 cat	0.130	0.987	0.350	0.960
150 cat	0.120	0.970	0.361	0.944

3.3.3 Influence of different initial concentration of dyes on initial rate constant

Figures 3.8 A and 3.8 B showed that the effect of initial concentration of dyes on degradation rate. It was observed that as the initial concentration of dyes (MO and RB) increases, percentage degradation decreases. The reason for this was the surface provided by the catalyst, intensity of the light and illumination times were constant. The numbers of adsorbing species on the catalytic surface were also constant. As the initial concentration increases, more and more amount of dyes was adsorbed on the surface of the photocatalyst depending on the surface provided by the catalyst. In such cases the $OH^{\cdot}$ and $O_2^{\cdot -}$ formed on the surface of the photocatalyst are also constant, so the strength of $OH^{\cdot}$ and $O_2^{\cdot -}$ Vs increasing concentration of dyes become less hence the photo-degradation efficiency decreases.

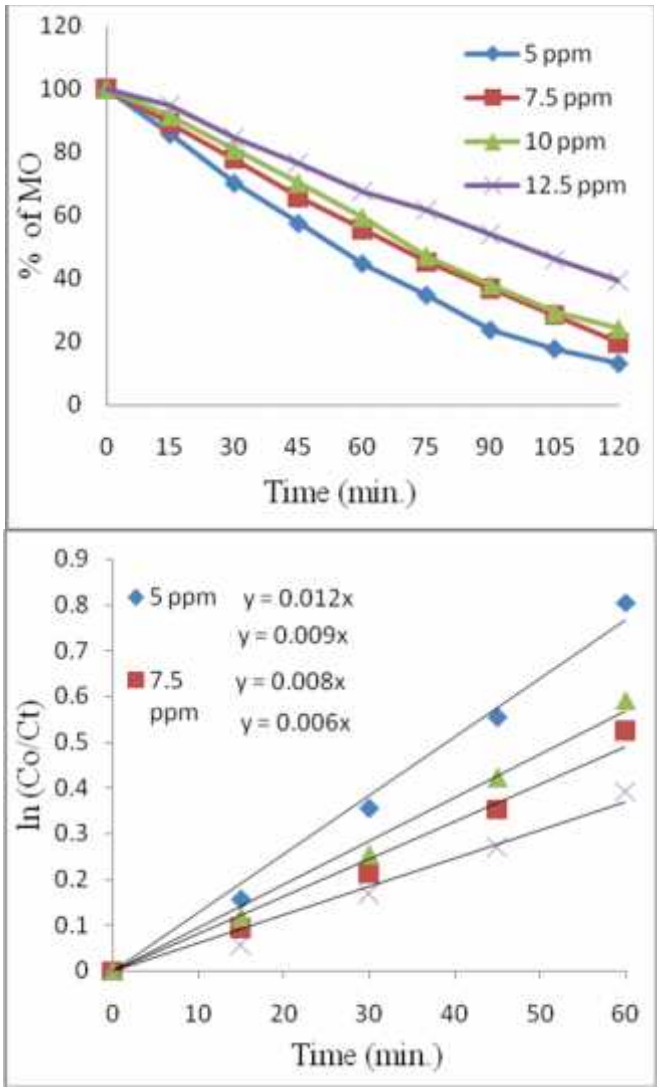

Figure 3.8-A Effect of different initial concentration of MO on degradation

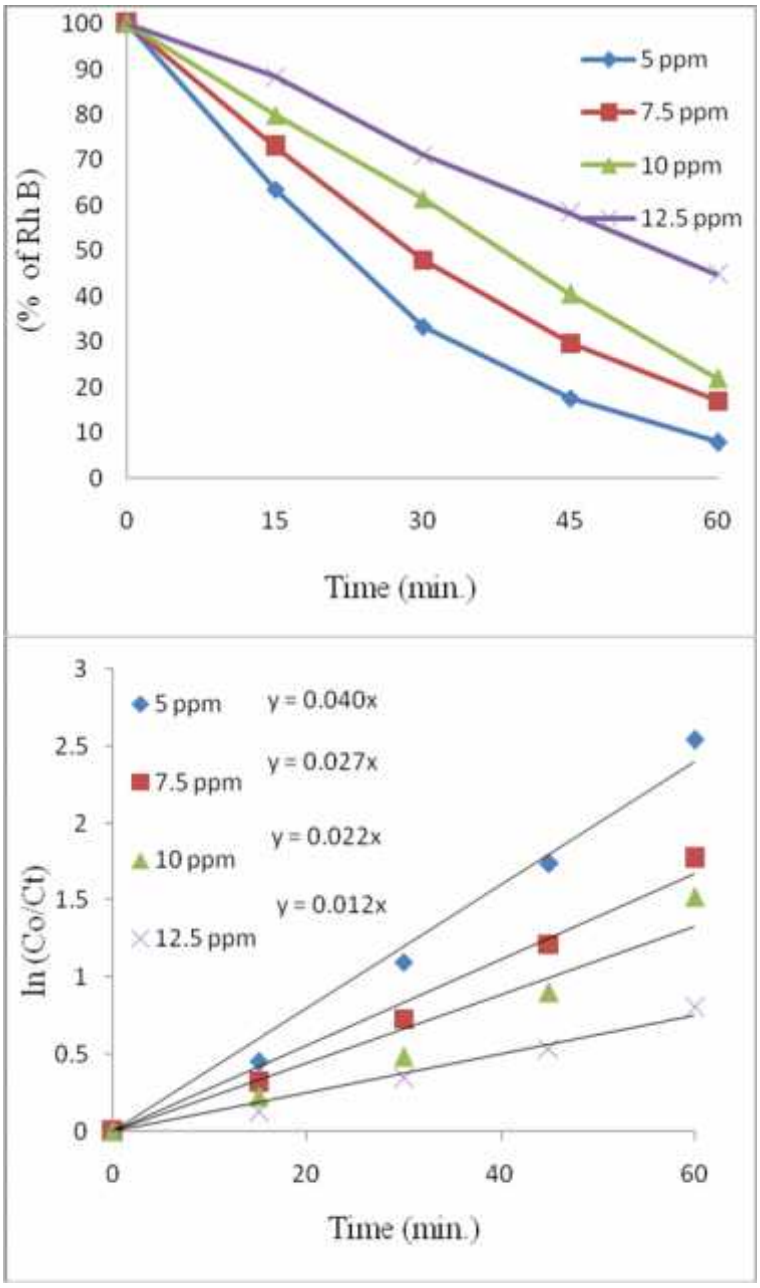

Figure 3.8-B Effect of different initial concentration of Rh B on degradation

3.3.4 Effect of different initial pH

Figure 3.9 shows the effect of initial pH on degradation rate of methyl orange and rhodamine b dyes. It was clear that the maximum degradation were observed at neutral pH whereas it decreases in acidic and alkaline medium. A remarkable increase in the %degradation of methyl orange and rhodamine b dyes was observed with increase in the pH ranging from 5 to 7. As ZnO is an amphoteric semiconductor, it dissolves in both acidic and basic medium. In acidic pH, ZnO gives corresponding salt and in alkaline pH, it forms complex like $[Zn(OH)_4]^{2-}$. ZnO shows low reactivity due to dissolution and photodissolution of ZnO in acidic and basic pH respectively [36].

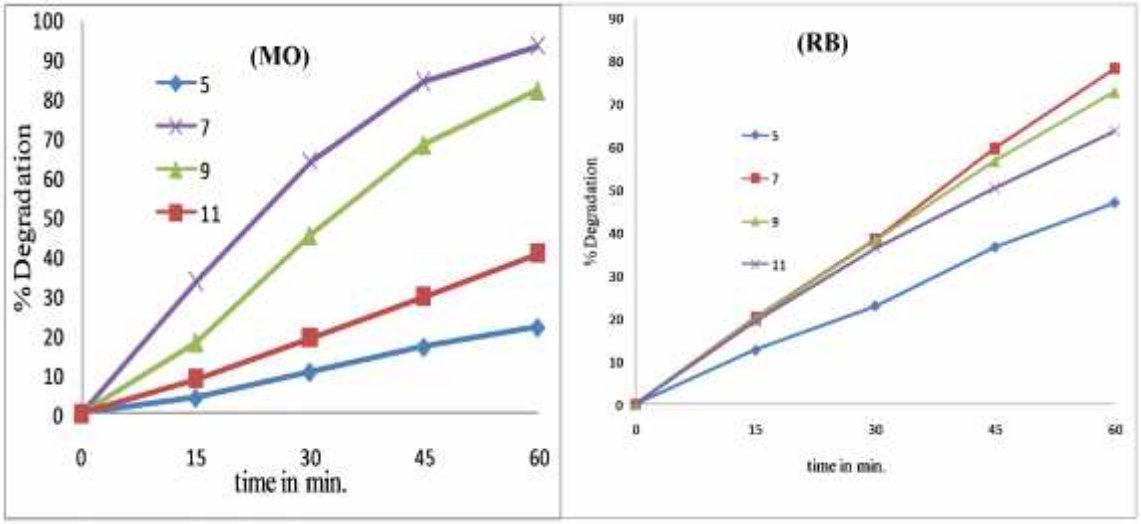

Figure 3.9 Effect of different initial pH on degradation of MO and Rh B dyes

3.3.5 Effect of various anions on degradation of MO and RB dyes

The study of the presence of trace amount of anions shows interesting results on the photodegradation rate of MO and RB dyes. Inorganic anions such as Cl^-, SO_4^{-2} and NO^{3-} have the tendency to get adsorbed on the surface of the catalyst by electrostatic attraction. They act as competitor against dissolved matter during adsorption. These inorganic anions affect the degradation rate by acting as hydroxyl radical scavenger and absorb UV light as well [25]. In order to investigate the effect of these inorganic anions on photo-degradation of MO and RB; an experiment is carried out to degrade 10 ppm of dye solution in presence of 0.5 mmol inorganic anion under irradiation system. The results were shown in table 3.3. In case of SO_4^{-2} ions, the degradation rate is greatly enhanced. Sulphate ions may react with $OH^{\bullet}$ radical which produces sulphate radical. As the strong oxidizing agent, sulphate radical can accelerate the photo-catalytic reaction [37].

$$SO_4^{-2} + OH^{\bullet} + H^{+} \longrightarrow SO_4^{\bullet -} + H_2O$$

Table 3.3 Effect of anions on degradation of MO and RB

Anions	Dye			
	MO		RB	
	k (min^{-1})	R	k(min^{-1})	R
No anion	0.149	0.988	0.372	0.954
Chlorine	0.057	0.998	0.288	0.990
Nitrate	0.074	0.995	0.227	0.994
Sulphate	0.161	0.987	0.425	0.952

Table 3.4 Optimized conditions for degradation of methyl orange and rhodamine b

Conditions	**Methyl orange / Rhodamine b**
Catalyst	3% MgO/ZnO
Catalyst Concentration	50 mg
Initial pH	Neutral
Favoured anoins	Sulphate

3.4 Conclusions

Photodegradation of methyl orange and rhodamine b dyes in water were studied using 3% MgO/ZnO photocatalyst. Some of the salient features of the photodegradation study are enlisted below:

- The present methodology does not require air or oxygen purging to achieve maximum degradation.
- Methyl orange and rhodamine b degrade efficiently with 3% MgO/ZnO photocatalyst by using 50 mg of the catalyst for maximum degradation.
- Degradation of dyes follows first order reaction kinetics.
- The maximum degradation was observed in neutral pH.
- The presences of sulphate anion increase the degradation rate.

3.5 References

1. R. W. Matthews, Water Res. 25 (1991) 1169-1176.
2. A. Sharma, P. Rao, R. P. Mathur, S. C. A. Ameta, J. Photochem. Photobiol. A: Chem. 86 (1995) 197-200.
3. S. Sakthivel, B. Neppolian, M. V. Shankar, B. Arabindoo, M. Palanichamy, V. Murugesan, Sol. Energy Mater. Sol. Cells 77 (2003) 65-82.
4. A. L. Linsebigler, G. Q. Lu, J. T. Yates, Chem. Rev. 95 (1995) 735-758.
5. T. L. Thompson, J. T. Yates, Chem. Rev. 106 (2006) 4428-4453.
6. S. K. Pardeshi, A. B. Patil, J. Mol. Catal. A: Chem. 308 (2009) 32-40.
7. S. Kim, W. Choi, J. Phys. Chem. B 109 (2005) 5143-5149.
8. G. K. Zhang, X. M. Ding, F. S. He, X. Y. Yu, J. Zhou, Y. J. Hu, J. W. Xie, Langmuir 24 (2008) 1026-1030.
9. D. Mijin, M. Savic, P. Snezana, A. Smiljanic, O. Glavaski, M. Jovanovic, S. Petrovic, Desalination 249 (2009) 286-292.
10. C. A. K. Gouvea, F. Wypych, S.G. Moraes, N. Duran, N. Nagata, P. Peralta, Chemosphere 40 (2000) 433-440.
11. C. Lizama, J. Freer, J. Baeza, H. D. Mansilla, Catal. Today 76 (2002) 235-246.
12. S. Amisha, K.Selvam, N. Sobana, and M. Swaminathan, Journal of the Korean Chemical Society 52 (2008) 66-72.
13. J. Bandara, S. S. Kuruppu, U. W. Pradeep, Colloids and Surfaces A: Physicochem. Eng. Aspects. 276 (2006) 197-202.
14. J. Bandara, K. Tennakone, P. P. B. Jayatilaka, Chemosphere 49 (2002) 439-449.
15. A. Hattori, Y. Tokihisa, H. Tada, S. Ito, J. Electrochem. Soc. 147 (2002) 2279-2283.
16. K. Vinodgopal, P. V. Kamat, Environ. Sci. Technol. 29 (1995) 841-845.
17. K. Tennakone, J. M. S. Bandara, O. A. Ileperuma, W. C. B. Kiridena, Semicond. Sci. Technol. 7 (1992) 432-435.
18. A. Mittal, A. Malviya, D. Kaur, J. Mittal, L. Kurup, J. Hazard. Mater. 148 (2007) 229-240.

19. S. D. Richardson, C. S. Wilson, K. A. Rusch, Ground Water 42 (2004) 678-688.
20. G. Li, Y. Ding, Y. Zhang, Z. Lu, H. Sun, R. Chen. J. of Col. and Inter. Sci. 363 (2011) 497–503.
21. Y. C. Zhang, Z. N. Du, K. W. Li, M. Zhang, Separation and Purification Technology 81 (2011) 101–107.
22. B. Zhao, F. Chen, Y. Jiao, H. Yang, J. Zhang, J. Mol. Cat. A 348 (2011) 114– 119.
23. L. Andronic, L. Isac, A. Duta, J. Photochem. Photobio. A 221 (2011) 30–37.
24. J. Haiyan, D. Hongxing, M. Xue, Z. Lei, D. Jiguang, J. Kemeng, J. Catal., 32 (2011) 939–949.
25. H. Zhang, P. Xu, G. Du, Z. Chen, K. Oh, D. Pan, Z. Jiao, Nano Res. 4 (2011) 274–283.
26. X. Li, Y. Hou, Q. Zhao, L. Wang, J. Col. Interf. Sci. 358 (2011) 102–108.
27. Z-D Meng, L. Zhu, J.-G Choi, C. Y. Park, W-C Oh, Ultrasonics Sonochemistry 19 (2012) 143–150.
28. F. Wanga, K. Zhangc, J. Mol. Catal. A 345 (2011) 101– 107.
29. J. Houa, R. Caoa, S. Jiao, H. Zhua, R.V. Kumar, App. Catal. B 104 (2011) 399–406.
30. T. S. Natarajan, M. Thomas, K. Natarajan, H. C. Bajaj, R. J. Tayade, Chem. Engg. J. 169 (2011) 126–134.
31. A. Mehrdad, B. Massoumi, R. Hashemzadeh, Chem. Engg. J. 168 (2011) 1073–1078.
32. H. Zhang, C. Hu, Cat. Commun. 14 (2011) 32–36.
33. J. Li, F. Sun, K. Gu, T. Wu, W. Zhai, W. Li, S. Huang, App. Cat. A 406 (2011) 51– 58.
34. O. W. Chun, C. Mingliang, C. Kwangyoun, K. Cheolkyu, M. Zeda, Z. Lei, J. Catal. 32 (2011) 1577–1583.
35. J. Cao, B. Luo, H. Lin, S. Chen, J. Mol. Cat. A 344 (2011) 138– 144.

36. E. Engenidou, K. Fytianos, I. Poulios, App. Cat. B: Environ. 59 (2005) 81-89.
37. S. Chen, G. Cao, Chemosphere 60 (2005) 1308-1315.